

# Operation regimes in a rotating detonation combustor

George Ionut VRABIE<sup>1</sup>, Daniel C. ASOLTANEI<sup>1</sup>, Andrei V. COJOCEA<sup>1</sup>,  
Mihnea GALL<sup>1</sup>, Ionut PORUMBEL<sup>\*,1</sup>, Alexa CRISAN<sup>1</sup>

\*Corresponding author

<sup>1</sup>National Research and Development Institute for Gas Turbines COMOTI,  
220D, Iuliu Maniu Bd., Bucharest, 061126, Romania,  
george.vrabie@comoti.ro

DOI: 10.13111/2066-8201.2025.17.1.8

Received: 31 August 2024/ Accepted: 09 September 2024/ Published: March 2025

Copyright © 2025. Published by INCAS. This is an “open access” article under the CC BY-NC-ND license (<http://creativecommons.org/licenses/by-nc-nd/4.0/>)

**Abstract:** *This paper presents an exploration of the operational envelope of a Rotating Detonation Combustor based on the design of the research group at the University of Southampton. The envelope is defined by hydrogen, respectively air feed line pressures between 2 and 10 bar. Three regimes have been identified: non-ignition, rotating detonation, and deflagration, and the limits, in terms of equivalence ratios have been determined. The discrimination between the three regimes was based on high speed static pressure measurements, infrared imaging, and acoustic evaluation. It has been found that detonation is characterized by a convergent flame in the near-field of the exhaust section, high pressure oscillations, and clear dominant frequencies in the kHz range, as well as by a characteristic loud, high-frequency sound.*

**Key Words:** *rotating detonation, supersonic combustion, experimental investigation*

## 1. INTRODUCTION

It has already been demonstrated by numerous studies [e.g. 1, 2] that thermodynamic cycles based on pressure gain heat addition to the working fluid offer an extraordinary potential in terms of cycle efficiency and a higher energy release rate. Various engine concepts that can accomplish this pressure supplement have been proposed over the years, and, among these, the Pulsed Detonation Engine (PDE), the Rotating Detonation Engine (RDE) and the Oblique Wave Detonation Engine (OWDE) are the most commonly studied. In all cases, a detonation wave is produced by igniting the combustible mixture under proper conditions. A detonation wave is composed of a leading shock wave coupled with a combustion wave, both travelling at the local speed of sound, where the leading shock wave raises the pressure and temperature of the fluid, allowing the combustion wave to propagate at the maximum possible velocity (called the Chapman – Jouguet velocity). The detonation wave causes an abrupt rise in pressure and temperature, fast enough to achieve complete combustion at a quasi-constant fluid density.

In OWDE [3, 4], the detonation wave is stabilized around an oblique shock wave, and the combustible mixture approaches it at supersonic speeds and ignites continuously, the burned gas being exhausted at hypersonic speeds. However, stabilizing this detonation wave remains an unsolved issue, the most recent [5] (2021) studies reporting a record 3 seconds of stable operation. In PDEs and RDEs, once created, the wave is free to travel through the engine at supersonic speed. The PDE [6, 7] is characterized by an unsteady cycle of a reactive mixture contained in a tube with a detonation wave created at one end, and traveling to the other end

of the combustor. The PDE cycle is started by filling the detonation chamber with a fuel/oxidizer mixture delivered through either a mechanical or aerodynamic valve, from the premixing area [1]. A detonation wave is initiated by means of a high-frequency ignition device, and combustion products are evacuated at the open end of the combustor, creating thrust [8]. Once the burned gases purged and the cycle repeats. The minimum cycle frequency to ensure performance above classical combustion (deflagration) is 75 Hz, and the state-of-the-art devices range between 100 and 400 Hz [9].

The RDE [10, 11] is characterized by a continuously operating process, where the detonation wave is created only once, being self-maintained by fresh reactants timely injected into the combustor. A high centrifugal force resulting from the tangentially propagating detonation wave is established, creating high radial pressure gradients that ensure the supply of fresh products into the chamber. Inertial forces trigger a rarefaction wave inside the annulus, helping burned gas evacuation and facilitating fresh products refill. The expanding detonation reactants that leave the annulus produce the engine thrust [12].

The afore mentioned advantages of the pressure gain combustion technology are revitalizing interest worldwide, particularly for space propulsion applications. Notably, NASA's recent RDE hot tests [13] in Huntsville confirmed its potential for deep space missions, aligning with parallel efforts at Purdue University led by Professor Guillermo Paniagua [10]. Moreover, JAXA recently achieved the first test of an RDE in space [14]. Likewise, there are various Russian [15], Korean [16] and Chinese [17] research groups that are contributing to the field. In Europe, contributions come from the "von Karman" Institute in Belgium [11], the Technical University of Berlin [18], and the Warsaw University of Technology [19].

The present paper presents an experimental assessment of the operating regimes appearing in a Rotating Detonation Combustor (RDC) as the feed fuel and oxidizer pressure vary.

## 2. METHODOLOGY

The RDC experimental model is based on the work carried out at the University of Southampton [20], optimized by our team by changing the critical section of the oxidizer stream and removing the need for a pre-detonator. A diagram of the RDC model is presented in Fig. 1.

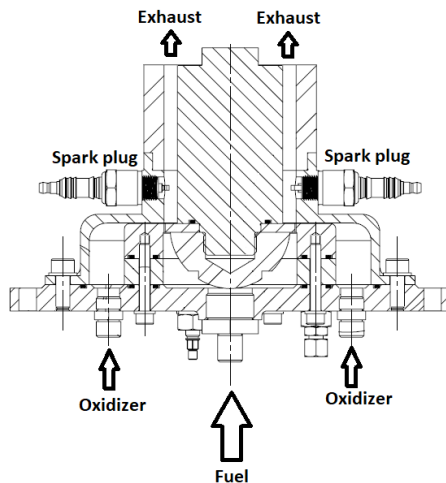


Fig. 1 – Diagram of the model RDC.

The RDC was installed on the Detonation and Rocket Engines Stand, part of the Testing and Experimentation centre for Space and Security of COMOTI, in Magurele, Ilfov. The test rig is capable of supplying air and oxygen at up to 11 bar, and gaseous fuel also up to 11 bar. Details of the test rig can be found elsewhere [9].

The measurements presented here were carried out using air as oxidizer and hydrogen as fuel, and the tests were performed at the oxidizer, respectively fuel feed line pressures given in Table 1. The instantaneous static pressure, measured in the horizontal plane that contains the spark plugs shown in Fig.1, but at a 90° angle to them, was measured using two Kulite ETM-HT-375 (M) high speed piezoelectric sensors. Along with this data, infrared images of the exhaust plume was captured using a FLIR Lepton 3.5 integrated into an iHunt Strong smartphone. Once ignition was achieved, the spark plugs were turned off during the measurements.

The two Kulite sensors were placed on the RDC model as shown in Fig. 2. The locations of other sensors are also presented in Fig. 2, but these data are outside the scope of the present paper, and should be disregarded.

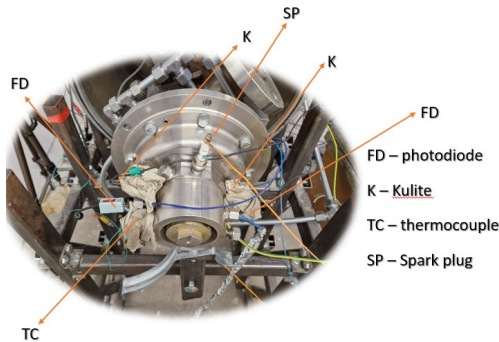


Fig. 2 – Location of sensors on the model RDC.

A full factorial Design of Experiment of the factors and levels presented in Table 1 has been conducted in order to explore the operating envelope map of the RDC, and to identify its operation regimes.

Table 1. – Test matrix

Factor	Level				
Oxidizer pressure [bar]	2	4	6	8	10
Fuel pressure [bar]	2	4	6	8	10

### 3. RESULTS

The operating envelope of the tested RDC was evaluated in terms of fuel and oxidizer feed pressures and equivalence ratio and is presented in Fig. 3. The equivalence ratio for each test case has been calculated based on the measured fuel and oxidizer mass flow rates, according to Equation (1). The equivalence ratio is defined as:

$$\varphi = \frac{\frac{\dot{M}_f}{\dot{M}_o}}{\left(\frac{\dot{M}_f}{\dot{M}_o}\right)_{st}} \quad (1)$$

where  $\dot{M}_f$  is the fuel mass flow rate,  $\dot{M}_o$  is the oxidizer mass flow rate, and the subscript  $st$  represents the stoichiometric conditions.

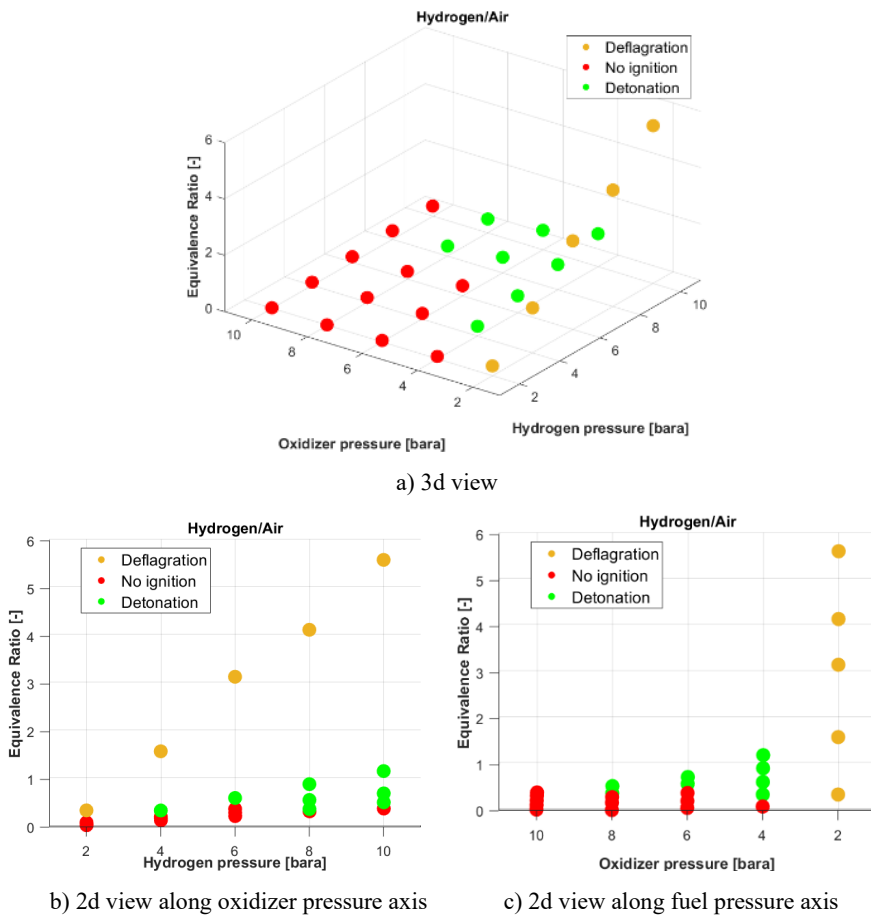


Fig. 3 – Operating envelope

The small mass flow variation at the same line pressure are artefacts of the experimental apparatus limitations. The line pressure could not be precisely set, only accurately measured. Therefore, the equivalence ratios are to be considered more relevant than the actual mass flow rates individually.

Three operating regimes were identified and summarized in Table 2: detonation, deflagration, and lack of ignition.

In Table 2, the cell colour indicates the regime: green for detonation, yellow for deflagration and red for lack of ignition. The white cell represents a borderline regime, between detonation and deflagration.

Table 2. – Operation regimes: The cells contain the values of the equivalence ratio

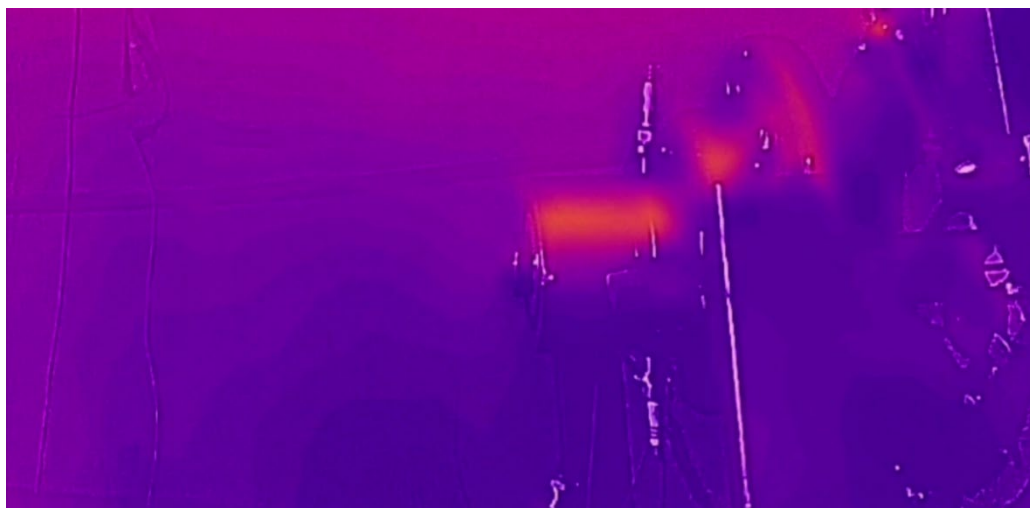
Pressure	H <sub>2</sub> / air					
	2 bar	4 bar	6 bar	8bar	10 bar	
2 bar	0.349	1.587	3.148	4.133	5.597	
4 bar	0.088	0.339	0.601	0.891	1.165	
6 bar	0.059	0.198	0.362	0.551	0.689	
8 bar	0.013	0.163	0.272	0.351	0.492	
10 bar	0.023	0.110	0.197	0.296	0.354	

For the extreme oxidizer pressures (i.e. 2 bar and 10 bar), no stable and sustained detonation regime is achieved, except for the borderline case. For the minimum (2 bar) hydrogen supply pressure, no stable detonation regime is reached as well (except for the borderline case again). In terms of equivalence ratio, all cases between 0.49 and 1.16 yield rotating detonation. In the range 0.33 - 0.49, some regimes yield detonation (4 bar air, 4 bar fuel and 8 bar fuel, 8 bar air), while other fail to ignite (6 bar air, 6 bar fuel and 10 bar fuel, 10 bar air). The 2 bar air, 2 bar fuel, also in this range, is the borderline case. It appears that in this region mixtures provided by oxidizer pressures above 4 bar, and fuel pressures below 8 bar fail to ignite. The region will have to be further investigated during the next experimental campaign. Below an equivalence ratio of 0.33, no ignition was recorded. Above an equivalence ratio of 1.58, the RDC operates in the deflagration regime. The region between an equivalence value of 1.16 and 1.58 was not explored and has to be tested in the future.

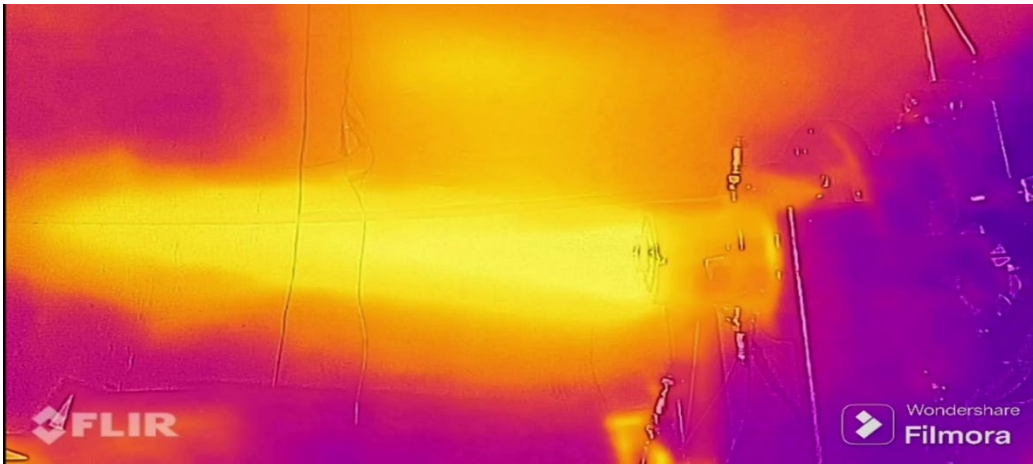
The discrimination between the deflagration and the detonation regimes was made by three methods: infrared imaging, pressure signals, and acoustic estimation. The infrared images for three representative cases for lack of ignition, deflagration, and detonation are presented in Fig. 4. The pressure signals and the Fast Fourier transforms of the same signals for three representative cases for lack of ignition, deflagration, and detonation are presented in Fig. 5, respectively Fig. 6. Infrared imaging was used instead of visible light imaging because the intensity of the light emitted by the hydrogen flame is quite low, and the details of the flame structure are hardly visible. Two lines (red and blue) are shown in Figs. 5 and 6, corresponding to each of the two sensors. The red line corresponds to the Kulite sensor on the left hand side of Fig. 2, while the blue line corresponds to the right hand side sensor.

The lack of ignition has been recorded for equivalence ratios above 0.354, irrespective of the air and fuel pressures. In this regime, no flame is visible at the RDE exhaust (Fig. 4a), and the recorded noise is very weak, and typical for low velocity jet noise.

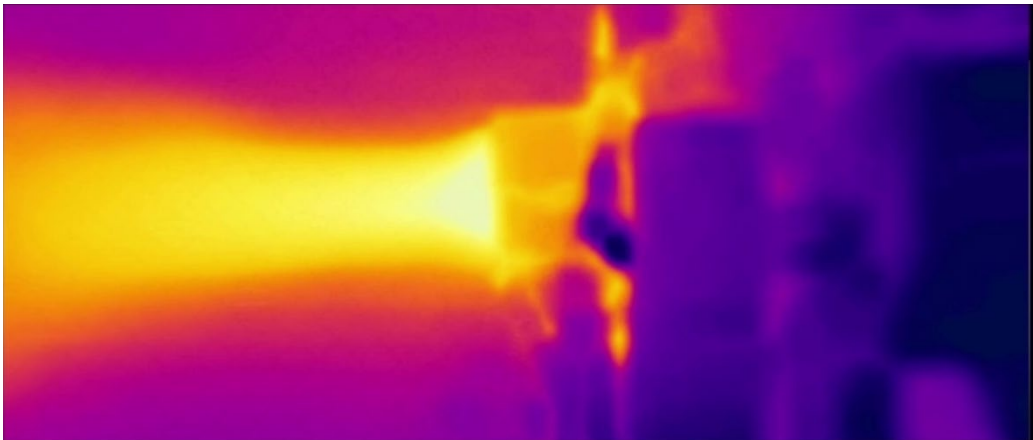
The recorded pressure signal presents some small fluctuations, likely due to turbulence (Fig. 5a). Consequently, the amplitude of the FFT peaks is small (Fig. 6a). The dominant frequency is high, and differs significantly for the two sensors (7 kHz, respectively 17 kHz). The identified frequencies are likely representing vortex shedding at the air inlet, and the difference between the sensors is probably related to geometrical imperfections in the assembly.



a) no ignition

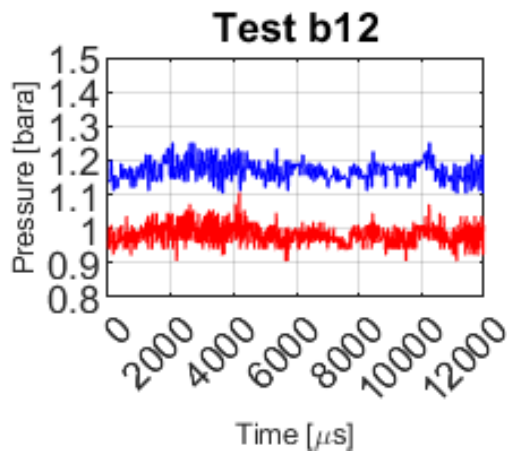


b) deflagration



c) detonation

Fig. 4 – Infrared imaging of representative cases for the RDC regimes.



a) no ignition

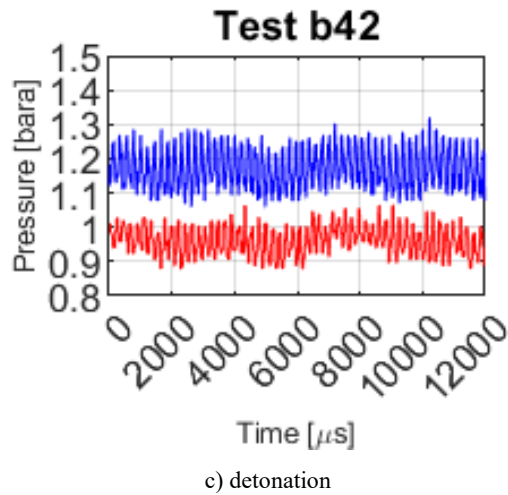
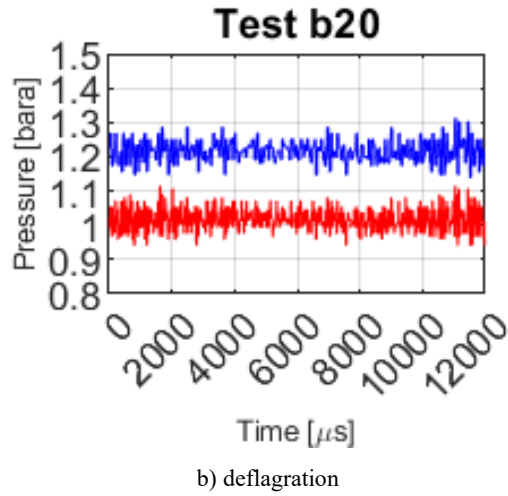
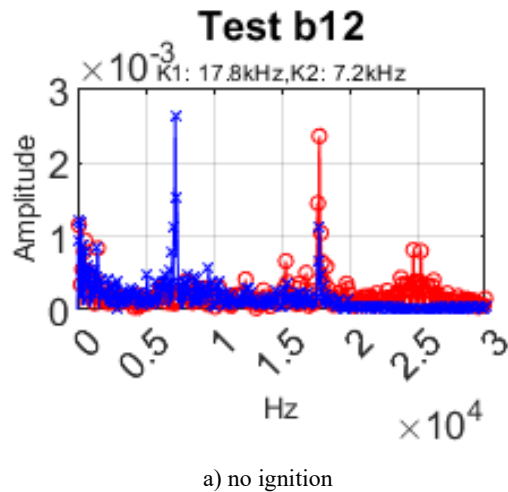
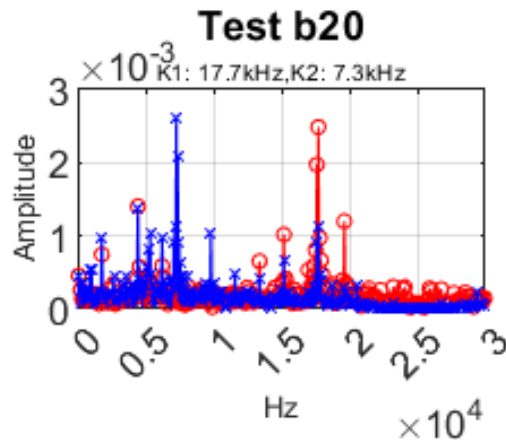
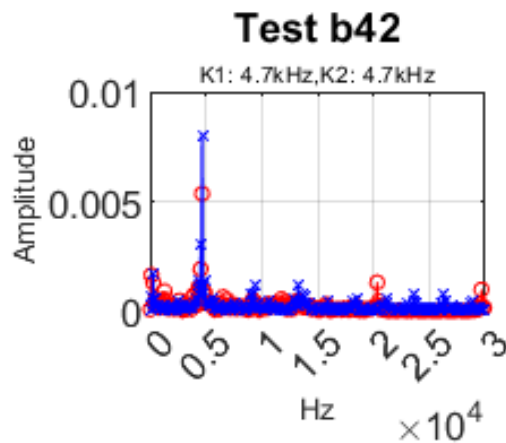


Fig. 5 – Pressure signal in representative cases for the RDC regimes





b) deflagration



c) detonation

Fig. 6 – Fast Fourier Transform of the pressure signal in representative cases for the RDC regimes

Deflagration regimes were observed for equivalence ratios below 0.088 and most of them occur at low air pressures (2 bar). A special case occurs when both the air, and the hydrogen line pressures are of 2 bar, which is borderline between deflagration and detonation (weak detonation). Here, the equivalence ratio is 0.349, significantly higher than for the other test cases where the airline pressure was set at 2 bar. The case will be analysed as a detonation case.

In these cases, a very long and visible turbulent flame can be seen at the exhaust of the RDC, as exemplified in Fig. 4b. The shape of the exhaust plume is divergent, as the hot gas is expanding in the atmosphere, downstream of the RDC exit section.

The perceived noise is significantly stronger than for the no-ignition case, and is low frequency. The recorded pressure signal, shown in Fig. 5b presents slightly larger variations in time, as the turbulence increases due to the dilatation and buoyancy effects caused by the deflagration heat release. No clear dominant frequency can be identified in the frequency space (Fig. 6b), and instead there are numerous low amplitude tones. The two dominant frequencies identified in the no ignition case and assumed to be related to vortex shedding are still visible and remain the highest amplitude tones in the analysis.

Detonation cases occur for equivalence ratios in the range 0.088 - 0.354. At the exhaust, the visible flame is much shorter than in the deflagration shape, and the shape of the exhaust plume is convergent - divergent, as shown in Fig. 4c. Immediately downstream of the RDC exhaust section, the plume is divergent, as the outward expansion wave velocity is limited by the speed of sound, while the axial convection velocity of the flame is supersonic. This is a clear indication of the supersonic nature of the flow and, hence, proof that the combustion developed in the detonation regime inside the RDC.

The noise produced by the RDC is much stronger, and has a much higher frequency. The pressure signal (Fig. 5c) shows strong and regular fluctuations in time, and the Fourier analysis of the signal (Fig. 6c) indicates dominant frequencies in the range of kHz. The amplitude of these dominant frequencies surpasses by an order of the magnitude the vortex shedding frequencies identified earlier.

#### 4. CONCLUSIONS

The operational envelope defined by oxidizer pressures between 2 and 10 bar, and fuel pressures between 2 and 10 bar also, has been explored, and three types of regimes have been identified by means of high speed static pressure measurements, infrared visualizations, and acoustic evaluation.

For equivalence ratios below 0.33, no ignition is recorded irrespective of the fuel and oxidizer pressures. Between 0.33 and 0.49 equivalence ratios values, the behaviour differs, the middle range pressure cases (6 bar for both air and hydrogen) failing to ignite, while the higher and lower pressures (4 and 8 bar for both air and hydrogen) are yielding detonation. The extremely low pressures (2 bar for both) result in weak detonation, while the extremely high pressure again fails to ignite. More research is needed in this range to understand the reasons for the observed behaviour.

Above an equivalence ratio of 0.49 but below 1.16, all cases yield stable rotating detonation, while equivalence ratios above 1.58 yield deflagration. The equivalence ratio range between 1.16 and 1.58 has not been explored and will be addressed by/in future experimental campaigns.

#### REFERENCES

- [1] K. Kailasanath, Review of Propulsion Applications of Detonation Waves, *AIAA Journal*, vol. **38**, no. (9), 2000.
- [2] C. F. Cuciumita, T. Cuciu and I. Porumbel, Evaluation of the Cycle Averaged Performances of PDE Based on Thermodynamic Cycle Computation, *GT2016 - 57310, ASME Turbo Expo*, Seoul, South Korea, 13-17 June, 2016.
- [3] G. P. Menees, H. G. Adelman and J.-L. Cambier, Analytical and Experimental Investigations of the Oblique Detonation Wave Engine Concept, *Technical Memorandum, National Aeronautics and Space Administration, NASA-TM-102839*, 1991.
- [4] Y. Liu, X. Han and Z. Zhang, Study on the propulsive performance of oblique detonation engine, *Energy*, vol. **292**, pp. 130519, 2024.
- [5] M. R. Thornton, D. Rosato, K. A. Ahmed, Experimental Study of Oblique Detonation Waves with Varied Ramp Geometries, *AIAA SCITECH 2022 Forum*, San Diego, CA, USA, 3-7 January, 2022.
- [6] T. Bussing and G. Pappas, An introduction to pulse detonation engines, *32nd Aerospace Sciences Meeting and Exhibit*, Reno, NV, USA, 10-13 January 1994.
- [7] P. Wolanski, Detonative Propulsion, *Proceedings of the Combustion Institute*, 34 (1), pp. 125-158, 2013.
- [8] A. Bogoi, T. Cuciu, A. V. Cojocea, M. Gall, I. Porumbel and C. E. Hrițcu, Experimental Pressure Gain Analysis of Pulsed Detonation Engine, *Aerospace*, vol. **11**, no. 6, pp. 465, 2024.
- [9] A. Cutler, Parametric Study of a High-Frequency Pulsed-Detonation Tube, *44th AIAA/ASME/SAE/ASEE Joint Propulsion Conference & Exhibit*, Hartford, CT, USA, 21-23 July, 2008.

- [10] V. Athmanathan, J. M. Fisher, Z. Ayers, D. G. Cuadrado, V. Andreoli, J. Braun, T. Meyer, G. Paniagua, C. A. Fugger and S. Roy, Turbine-integrated High-pressure Optical RDE (THOR) for injection and detonation dynamics assessment, AIAA 2019-4041, *AIAA Propulsion and Energy 2019 Forum*, Indianapolis, IN, USA, 19-22 August, 2019.
- [11] B. H. Saracoglu and A. Ozden, The effects of multiple detonation waves in the RDE flow field, *Transportation Research Procedia*, vol. **29**, pp. 390-400, 2018.
- [12] F. K. Lu and E. M. Braun, Rotating Detonation Wave Propulsion: Experimental Challenges, Modeling, and Engine Concepts, *Journal of Propulsion and Power*, vol. **30**, no. 5, pp. 1125-1142, 2014.
- [13] T. W. Teasley, T. M. Fedotowsky, P. R. Gradl, B. L. Austin and S. D. Heister, Current State of NASA Continuously Rotating Detonation Cycle Engine Development”, *AIAA SCITECH 2023 Forum*. 23-27 January, National Harbor, MD, USA, 2023.
- [14] H. Watanabe, K. Matsuyama, K. Matsuoka, A. Kawasaki, N. Itouyama, K. Goto, K. Ishihara, Kazuki & V. Buyakofu, T. Noda, S. Ito, K. Kasahara, A. Matsuo, I. Funaki, D. Nakata, M. Uchiumi, H. Habu, S. Takeuchi, S. Arakawa, J. Masuda and K. Yamada, Flight Demonstration of Detonation Engine System Using Sounding Rocket S-520-31: Flight Path and Attitude, *AIAA SCITECH 2022 Forum and Exposition*, 3-7 January, San Diego, CA, USA, 2022.
- [15] S. M. Frolov, V. S. Aksenov, V. S. Ivanov, S. N. Medvedev and I. O. Shamshin, *Flow Structure in Rotating Detonation Engine with Separate Supply of Fuel and Oxidizer: Experiment and CFD*, In: J.M. Li, C. Teo, B. Khoo, J.P. Wang and C. Wang (Eds.), *Detonation Control for Propulsion, Shock Wave and High Pressure Phenomena*. Springer, 2018.
- [16] H. S. Han, E. S. Lee and J. Y. Choi, Experimental Investigation of Detonation Propagation Modes and Thrust Performance in a Small Rotating Detonation Engine Using C<sub>2</sub>H<sub>4</sub>/O<sub>2</sub> Propellant, *Energies*, 2021.
- [17] Z. Rui, W. Dan and J. P. Wang, Progress of continuously rotating detonation engines, *Chinese Journal of Aeronautics*, vol. **28**, no.1, pp. 15-29, 2016.
- [18] R. Bluemner, M. D. Bohon, C. O. Paschereit and E. J. Gutmark, Experimental Study of Reactant Mixing in Model Rotating Detonation Combustor Geometries, *Flow, Turbulence and Combustion*, vol. **102**, no. 2, pp. 255 – 277, 2019.
- [19] M. Kawalec, P. Wolanski, W. Perkowski and A. Bilar, Development of a Liquid-Propellant Rocket Powered by a Rotating Detonation Engine, *Journal of Propulsion and Power*, vol. **39**, no. 4, pp. 554 – 561, 2023.
- [20] H. Law, T. Baxter, C. Ryan and R. Deiterding, Design and testing of a small-scale laboratory rotating detonation engine running on ethylene-oxygen, *AIAA Propulsion and Energy 2021 Forum*, August 9-11, 2021.